Multi-wavelength studies of accretion phenomena with SALT and ASTROSAT

David A.H. Buckley[1] and Kulinder Pal Singh[2]

[1] Southern African Large Telescope, PO Box 9, Observatory 7935, Cape Town, South Africa, e-mail: `dibnob@salt.ac.za`
[2] Tata Institute of Fundamental Research, 1 Homi Bhabha Road, Colaba, Mumbai 400005, India

Abstract. The Southern African Large Telescope (SALT) is a 10-m ground-based optical-IR telescope which has a range of instrumentation ideally suited to observe a variety of phenomena in astrophysical objects powered by accretion, from binary stellar systems (involving white dwarfs, neutron stars and black holes), to Active Galactic Nuclei. SALT's observational capabilities include time resolved optical photometry, spectroscopy and polarimetry, down to sub-second time resolution. ASTROSAT will be India's first astronomy satellite and will carry an array of instruments capable of simultaneous observations in a broad range of wavelengths: from the visible, near ultraviolet (NUV), far-UV (FUV), soft X-rays to hard X-rays. We plan to harness the capabilities of both observatories to undertake contemporaneous multi-wavelength observations of the various classes of accretion driven variable X-ray sources. By observing in both the optical (SALT), ultraviolet and X-ray regimes (ASTROSAT), we will correlate the spectral energy distributions, fluxes and spectral variations for a variety of objects.

Key words. Accretion, Cataclysmic Variables, X-ray binaries, AGN, X-rays and UV, X-ray Telescopes, UV Telescopes, X-ray and UV Detectors, ASTROSAT, Astronomy Satellite

1. Introduction

SALT (Buckley et al. 2006a) is one of five 10-m class segmented mirror telescopes - the only one situated in the southern hemisphere – and is closely modelled on the Hobby Eberly Telescope (HET) in Texas. Full science operations with SALT began in late 2011 with two first generation instruments, the Robert Stobie Spectrograph (RSS) and the SALTICAM imaging camera, both mounted at the f/4.2 prime focus. A third instrument, the fibre-fed High Resolution Spectrograph (HRS), was installed in 2013. Some of the science drivers which dictated the instrument designs for both RSS and SALTICAM, included the ability to undertake time-resolved studies, at timescales as short as ~0.1 sec, particularly to study the rapid flux and spectral variability in accreting binary stars (e.g. cataclysmic variables, X-ray binaries and related objects). In addition, polarimetric (imaging and spectro polarimetry) capabilities were designed into RSS, plus the ability to observe down to the UV cutoff of the atmosphere. Finally, because of SALT's design, all observations are queue scheduled, which makes it easier to conduct monitoring or synoptic observations, spaced

over timescales of days, weeks and months, which can be used to study the changing behaviour of different accretion powered objects on the timescales associated with the mass transfer or dynamics of the systems (e.g. orbital period for binary systems).

Remarkable progress has been made in X-ray and Ultraviolet (UV) astronomy in the last 5 decades with the launch of an impressive array of detectors and telescopes on several satellite missions. These windows provide an incisive insight into the radiation mechanisms and the environments of cosmic sources, particularly accretion powered objects which emit a significant fraction, perhaps most, of their luminosity in X-rays. Understanding the radiation from these sources, however, requires a wide coverage over the entire electromagnetic spectrum. Since these radiations are also variable on a variety of time scales, simultaneous measurements over a wide range of wavelengths have become one of the essential requirements.

ASTROSAT will be India's first multi-wavelength astronomy satellite when it is launched in the first half of 2015. With its suite of several co-aligned instruments, ASTROSAT has been designed to carry a range of wideband X-ray instruments with overlapping energy response and UV detectors for simultaneous spectral and temporal studies to identify and quantify contributions of different components (e.g. thermal, non-thermal, black body, synchrotron, inverse-Compton, spectral lines) in X-ray sources, and thus to understand their nature and astrophysical processes in them. There are no other international observatories planned in the near future that can cover the entire X-ray spectral band from 0.3 to 100 keV and the UV bands from 1300 - 3000 Angstroms in one mission. Equipped with instruments in these bands, ASTROSAT will thus be a unique mission to address a host of scientific issues in X-ray and UV astronomy.

2. The coordinated SALT-ASTROSAT observing program

This observing program is planned to begin during the Performance Verification (PV) and Guaranteed Time Observation (GTO) phases of ASTROSAT, expected to extend over ~12-18 months, and eventually extend to the Guest Observer (GO) phase. A variety of objects, covering representative samples of source classes, will be chosen for contemporaneous ground-based observations, particularly with SALT, but also other ground-based observatories in both the optical and radio, where appropriate (e.g. IAO, SAAO, GMRT, KAT7 & eventually MeerKAT). Multi-wavelength variability on a range of timescales, from the sub-second to longer (i.e. weeks/months), will be investigated to better understand the nature of accretion state changes and the consequent effect on the observed characteristics of individual objects through their spectral energy distributions, spin and orbital modulations, emission line diagnostics and optical/UV/X-ray light curves. ASTROSAT will provide X-ray spectra (e.g. from the SXT, LAXPC and CZTI instruments; see subsequent sections) and, in certain circumstances, simultaneous UV/optical imaging. The SSM instrument will detect transient X-ray sources. SALT will provide full near UV-optical spectral coverage at resolutions from R ~500 – 9000, potentially at high time resolution and including polarimetric measurements, where appropriate.

SALT, with its suite of instruments, is especially well suited to multi-wavelength and time resolved studies of astronomical objects, and particularly the objects proposed for the ASTROSAT PV and GTO phases. The queue scheduled nature of SALT's operation will allow us to conduct synoptic monitoring observations of variable objects on a variety of timescales. We therefore expect to advance our understanding of a whole range of objects, including cataclysmic variables (magnetic and non-magnetic), novae and recurrent novae, low and high mass X-ray binaries, X-ray transients, stellar mass black holes and black holes associated with AGN and galactic nuclei. The results of the program will include studies on both individual systems and, longer term, population studies of object classes.

ASTROSAT will be a significant new X-ray astronomy facility, boasting a large effective collecting area in hard X-ray and with a significantly higher energy response than pre-

vious missions. This has distinct advantages in the study of hot thermal plasmas, which are ubiquitous amongst accretion powered objects, which are some of the most energetic objects in the Universe. The LAXPC instrument will help to constrain the temperature of the hard thermal bremsstrahlung components emitted by such objects as magnetic CVs, accreting neutron stars (e.g. in LMXBs) and black holes. Another key strength of ASTROSAT will be its ability to discover and locate transient X-ray sources, using the Scanning Sky Monitor. Such a capability is key to the on-going studies of such objects as soft X-ray transients, X-ray nova and other eruptive events (e.g. novae). With the end of the RXTE facility (in 2011), the ability of detecting X-ray transients has been seriously curtailed and ASTROSAT is key for on-going transient discoveries.

Observations with ASTROSAT will provide sorely needed new X-ray data. However, it is only through comprehensive optical observation (ideally contemporaneous) that a complete picture can emerge. We therefore plan to utilize SALT in order to undertake appropriate observations as near as possible to the ASTROSAT observing times. Some compelling aspects of simultaneous observations hinge on the rare or unique capabilities of SALT in terms of high time resolution studies, particularly for targets of opportunity (ToOs), like for transient X-ray sources. Because of SALT's 100% queue scheduled operation, it is relatively easy to schedule contemporaneous or simultaneous observations in support of ASTROSAT. Such data could address the often seen delays between X-ray and optical flux variations, either as a result of accretion related emission at different locations in a source, or due to radiation reprocessing. Objects from the following X-ray source classes will be observed as part of these planned coordinated observations with ASTROSAT, SALT and, in some cases, other ground-based facilities.

2.1. Magnetic Cataclysmic Variables (mCVs)

X-rays from the accretion shocks just above the white dwarf surface and surrounding re-

gion will be detectable by ASTROSAT's instruments (e.g. LAXPC, SXT and in some instances, the CZTI) and in some cases so will the UV emission from thermalized X-rays and blobby accretion (by the UVIT). Observations of newly identified (e.g. from the INTEGRAL and Swift satellites) and under-studied mCVs are therefore planned during the PV & GTO phases in order to model their X-ray spectra and study the spin and orbital modulations. Contemporaneous SALT observations, particularly high-speed photometry and time resolved spectroscopy, polarimetry and spectropolarimetry, will assist in defining comprehensive multi-wavelength models for these systems. The SALT (& other optical) data will probe the dominant cyclotron cooling of the accretion columns and the regions where X-rays are reprocessed into UV-visible photons, deriving fundamental information on the magnetic fields and plasma properties. Studies of quasi-periodic oscillations (QPOs), arising from accretion instabilities, will also benefit from contemporaneous optical and X-ray observations.

2.2. Low mass X-ray binaries

Accretion disks are ubiquitous in a wide range of astronomical systems (proto-stars, cataclysmic variables, X-ray binaries and AGN), so understanding their structure and physics is a key requirement to explain several observational aspects, as well as to probe extreme physics near neutron stars and black holes. Thermonuclear X-ray bursts, originating from intermittent and unstable thermonuclear burning of accreted matter accumulated on the surfaces of some neutron stars in LMXBs, provide a potentially excellent way to map the structures of large portions of accretion disks. ASTROSAT will be particularly useful for time-resolved spectroscopy of bursts, providing a broad X-ray spectrum of the illuminating radiation. Simultaneous SALT observations can provide additional optical information at much better sensitivity and time resolution (e.g. compared to UVIT alone). Furthermore, a portion of the illuminating radiation may be reprocessed from the compan-

ion star, and this reprocessed radiation should be modulated with the binary orbital period, which SALT may be able to detect.

2.3. Eruptive variables: novae and supernovae

Multi-wavelength monitoring of classical and recurrent novae during outburst are planned using the ASTROSAT (X-ray and UV), GMRT, KAT7 & (eventually) MeerKAT (Radio) and HCT, SALT (optical and NIR) facilities. Such observations will provide a comprehensive, multi-wavelength dataset of the outburst that will be of prime importance for theoretical models of the outburst and its evolution. While the UV data and optical/NIR data would provide early outburst energetics, the X-ray and radio will provide information about the later phases, and interaction with circumstellar medium. X-ray data, especially in the (relatively rare) super-soft (SSS) phase will provide clues to the mass of the white dwarf. The regular optical and UV monitoring observations, afforded by SALT and other ground-based optical facilities, would thus help in scheduling the optimal time of X-ray observations using ASTROSAT during the SSS phase.

2.4. X-ray transients

The deactivation of the NASA Rossi X-ray Timing Explorer (RXTE) satellite in late-2011 significantly reduced the ability for astronomers to detect new X-ray transients, which invariably harbor interesting accretion driven sources (e.g. black hole systems, microquasars, supergiant fast X-ray transients, soft X-ray transients) providing a rich sample of new observational phenomena. ASTROSAT, through the Scanning Sky Monitor (SSM) instrument, will provide a new capability for the detection of such transients and it is expected that follow-up observations of transients will be a key ASTROSAT science program. Simultaneous ASTROSAT and SALT observations will be undertaken where possible through Target of Opportunity (ToO) programs, similar to ones already attempted us-

ing the RXTE, SWIFT, MAXI, Suzaku, XMM-Newton and Chandra X-ray facilities.

The Galactic soft X-ray transients (SXTs) provide unique insights into the properties of (stellar-mass) black hole and neutron star X-ray binaries. Most are optically too faint in quiescence for a detailed study of the mass donor, so we must instead extract the crucial kinematic information during X-ray outburst. While the disk dominates in the optical during outburst, it is possible to spectroscopically resolve the sharp Bowen fluorescence lines, formed on the donor's X-ray heated face. Such features can provide extremely accurate velocity information about the donor, and the broad disc lines provide other constraints. Coordinated ASTROSAT and SALT observations of such transients will be conducted in order to simultaneously derive their X-ray and optical properties, including determinations of the orbital periods. Fast optical photometry with SALT, simultaneous with ASTROSAT, on other transient systems will be used to determine lags between the X-ray and optical light curves, leading to determinations of system dimensions.

2.5. Active Galactic Nuclei

Active galactic nuclei (AGN) are amongst the most luminous discrete sources in the Universe, as bright as an entire giant galaxy, but very compact, only about the size of the solar system. AGN show flux variations over the entire electromagnetic spectrum and over a wide range of timescales and amplitudes. Studying variability over different wavelengths helps to understand the relationship between different physical regions of AGN. It is now believed that super-massive black holes (SMBHs) are ultimately responsible for the phenomena associated with AGN. X-ray observations of AGN, as will be afforded by ASTROSAT, are a key element in understanding their nature. Such observations probe the regions of AGN that are close to the central SMBH, where accretion is taking place. Optical variability has been attributed to either X-ray reprocessing, or alternatively the X-rays are a result of Compton scattering of optical

photons. Either way, variability lags are expected (and seen) between X-ray and optical light curves, which we aim to detect in other objects.

Unraveling the physics of AGN demands simultaneous X-ray and optical observations, which has not hitherto been easily achieved due to difficulties in co-ordinating observations. We aim to overcome this limitation by efficiently observing selected targets using the X-ray and UV/optical capabilities of ASTROSAT, supplemented with more detailed SALT (& other ground-based) optical observations. The structure of AGN on the smallest possible scales can potentially be probed through the process known as reverberation mapping, which uses the intrinsic variability of the nuclear continuum source and the light-travel time-delayed response of the broad emission-line gas to these variations. ASTROSAT will detect AGN which show increased X-ray flux states and reverberation studies will then be initiated through regular SALT spectroscopic monitoring. Similar programs have been successfully carried out on SALT, but ASTROSAT will enable a wider selection of potential targets.

Parallel to these AGN observations, we also plan to observe X-ray bright normal galaxies (XBONGs), first found by the Einstein X-ray observatory and subsequently by other X-ray missions. A clear understanding of these objects is still elusive and while their X-ray luminosities require accretion on to compact objects, the absence of tell-tale optical signatures could be due to a variety of reasons. ASTROSAT could discover many more XBONGs which, though bright in X-rays, are optically less luminous and thus optical observations require 10 m class telescopes – like SALT.

3. SALT instruments

The four science instruments on SALT currently comprise:

1. SALTICAM, a broad-band UV-visible imaging camera (Buckley et al. 2006a,b).
2. RSS, the Robert Stobie Spectrograph, formerly known as the Prime Focus Imaging

Fig. 1. The 10-m SALT

Spectrograph (PFIS) (Buckley et al. 2006b; Burgh et al. 2003).
3. SALT HRS, a fibre fed high resolution échelle spectrograph, primarily designed for bright single objects (Barnes et al. 2008; Barmall et al. 2010).
4. BVIT, the Berkeley Visible Image Tube photon counting camera, a visitor instrument (Buckley et al. 2006b).

The first two instruments were completed in 2005 and installed on SALT prior to inauguration and are now referred to as the SALT "first light" instruments. The third, SALT HRS, had both technical and funding difficulties, which caused a significant delay in its development. The design phase of SALT HRS was completed in 2005 by another SALT partner, the University of Canterbury, and the instrument was built by Durham University's Centre for Advanced Instrumentation and was installed on SALT in 2013.

A brief overview of the SALT instrument capabilities are now given, with some emphasis on those relevant to the study of accretion powered sources as already reviewed in Section 2.

3.1. SALTICAM

SALTICAM is a multi-purpose device, capable of performing roles as both an efficient acquisition and guidance camera and a scientific imager (Buckley et al. 2006a,b). The instrument images onto two mosaiced E2V 44-82 frame transfer deep depletion CCDs ($2048 \times 4096 \times 15\mu m$ pixels), giving a field of $\sim 10 \times 10$ arcmin). SALTICAM's optics are designed to allow observations down to the UV atmospheric cut off (~ 320 nm). The current filter sets include Johnson-Cousins (UBVR$_c$I$_c$), Strömgren and Sloan filters, plus some customized narrow band (FWHM $\sim 20 - 40$ nm) filters in the UV (340 & 380 nm) and the red (610, 705, 815 & 860 nm). SALTICAM employs frame transfer CCDs, which allows for fast acquisition and imaging. For frame transfer mode, with 2 x 2 binning, the shortest exposures are ~ 2.5 sec.

A special high-speed photometry mode, known as "slot mode", allows for just a small region of the CCD to be illuminated by moving an occulting mask with a narrow slot (~ 20 arcsec wide) to just above the frame transfer boundary (i.e. between the image and store arrays). This illuminated region of the CCD is then quickly (typically ~ 3ms) row-shifted into the storage array, while another exposure begins. A target object, and local comparison star(s), can then be placed in the slot to allow for high-speed (down to ~ 80 ms time resolution, determined by the minimum readout time) differential photometry. This mode has been used to study high frequency variability in CVs and X-ray binaries and will be exploited in our program of contemporaneous SALT-ASTROSAT observations of such objects.

3.2. RSS

This instrument is the main work-horse instrument on SALT and resides at the prime focus, where it takes advantage of the direct access to

the focal plane, maximizing efficiency over the wavelength range of the instrument, namely 320 – 900 nm and avoiding the use of optical fibres. In addition it was designed to have a range of capabilities and observing modes, each one remotely and rapidly reconfigurable (Buckley et al. 2006b). In keeping with the overall philosophy of exploiting the niche areas where SALT has a competitive edge, the instrument has several unique, or rare, capabilities for a large telescope, some afforded by various enabling technologies in the area of efficient anti-reflection coatings, gratings and detectors. The capabilities of RSS include:

1. The ability to observe down to the UV atmospheric cut-off, at ~ 320 nm. This is achieved by the judicious use of UV transmitting materials in the all-refractive optical design, including fused silica, fused quartz, CaF$_2$ and NaCl (the latter used as central elements in sealed triplets). High throughput has demanded the use of efficient anti-reflection coatings, including Solgel on interior (sealed) lens surfaces.

2. Low to medium resolution spectroscopy (R $\sim$ 500-5500 with 1" slits; R $\sim$ 10000 with 0.6" slits) using five tuneable VPH gratings (900, 1300, 1800, 2300 & 3000 lines mm^{-1}) and one transmission grating (300 lines mm^{-1}).

3. All Stokes mode spectropolarimetry and imaging polarimetry using either one or both 1/2 and 1/4 waveplate retarders and a large Wollaston beam-splitter mosaic, giving two completely off-set O- and E-images on the detector. High-speed and simultaneous modes will also be available, which is particularly pertinent for time varying polarized sources.

4. Fabry-Perot imaging spectroscopy in the range 430-860 nm using three etalons, in dual mode for medium and high resolution, providing three resolution regimes of R = 320–770, 1250– 1650 and 9000.

5. The use of fast frame-transfer CCDs allowing for high-speed observations in all observing modes.

RSS has been used to conduct time resolved spectroscopy of accretion driven bina-
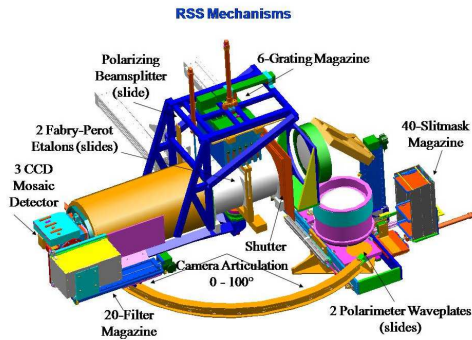
Fig. 2. Schematic of the SALT Robert Stobie Spectrograph (RSS)

ries (CVs, LMXBs) and AGN (reverberation mapping), as well as spectropolarimetric observations of mCVs and a Recurrent Nova in outburst (T Pyx). Similar observations will be undertaken as part of this program.

3.3. HRS

This instrument is a fibre-fed high resolution (from R ~ 16,000 to 80,000), depending on fibre/slicer choice) vacuum echelle spectrograph, designed for precise radial velocity stability, as needed for exo-planet studies. Although the instrument is really designed for brighter objects (V < 16), it has been used to observe novae and other bright transient phenomena, and will be used accordingly for appropriate targets in our program.

3.4. BVIT

This visitor instrument is currently made available by the Space Science Lab at UC-Berkeley, specifically to study variability at very high time resolution (i.e. down to μsec time resolution). It employs a Micro Channel Plate (MCP) and strip anode detector, enabling photon counting measurements to be made by time tagging photon arrival times to ~50ns. The instrument has been successful in observing the optical pulses from the 51 ms pulsar, PSR B0540-69, as well as number of CVs and flare stars. For appropriately objects, we plan to utilize BVIT in our program.

4. ASTROSAT's performance parameters

ASTROSAT will be launched into a circular 650 km orbit with an inclination of ~6 degrees and will have a 97 min orbital period, with the Sun being eclipsed for ~35 min. The total mass of the satellite is estimated to be 1550 kg including 780 kg mass for the scientific instruments. ASTROSAT will be a three-axis stabilized satellite and will have target acquisition capability of ~30 arcsec and, by correction with star sensors, it will be able to achieve a pointing accuracy of ~1 arcsec. A solid-state recorder with 200 Gb storage capacity will be used for on-board storage of data, which is enough to record data for four orbits. The data will be transmitted via two phased array antennas with 5-6 ground station contacts per day. The satellite's positioning system will provide a time reference to ~200 ns accuracy. A large number of heaters and sensors will provide thermal control of all the payloads and subsystems as specified by each subsystem. ASTROSAT will have a nominal lifetime of about 5 years.

The spacecraft will carry five principal scientific instruments: (i) a Soft X-ray Telescope (SXT), (ii) three Large Area Xenon Proportional Counters (LAXPCs), (iii) a Cadmium-Zinc-Telluride Imager (CZTI), (iv) an Ultra-Violet Imaging Telescope (UVIT) configured as two independent telescopes, and (v) a Scanning Sky Monitor (SSM). A summary of the basic scientific performance parameters of these payloads is given in Table 1. A schematic diagram of the satellite (in stowed position) with all the payloads is shown in Fig. 3.

The basic performance parameters of ASTROSAT are listed in Table 1. Imaging in the ultra-violet regime has a spatial resolution of 1.8 arcsec (~3 times better than GALEX) in a fairly wide field of ~ 28 arcmin. The effective area of LAXPC for energies above 30 keV is several times larger than that of the RXTE, making it the most sensitive detector in the energy range of 30 – 80 keV. The LAXPC has the highest time resolution of all the ASTROSAT instruments. It is also more sensitive to the de-
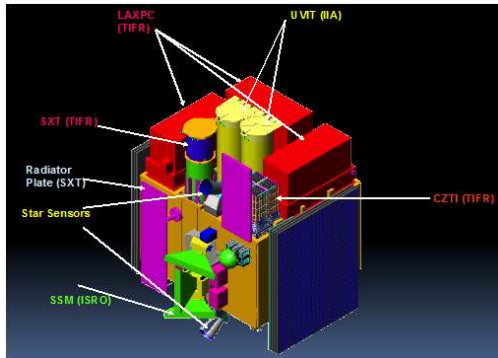
Fig. 3. ASTROSAT in a stowed position showing the science instruments.

Fig. 4. Left: Integrated SXT with all major parts; Right: Optics assembly of all the mirrors for the SXT.

tection of Fe lines in the 6 – 7 keV energy band than the SXT, though with a lower energy resolution. SSM will scan a large portion of the sky every few hours to detect and locate transient X-ray sources in the outburst phase, in the 2.5 -10 keV energy range.

5. ASTROSAT instruments

5.1. Soft X-ray Telescope (SXT)

The SXT consists of a set of coaxial and confocal shells of conical mirrors approximating paraboloidal and hyperboloidal shapes and arranged behind each other in a geometrical arrangement known as approximate Wolter I optics. Nesting of Wolter I shells is incorporated to improve the effective area. SXT has 40 complete shells of mirrors assembled quadrant-wise (total of 320 mirrors) in a grooves and spokes arrangement, similar to that used in the Danish X-ray telescope made for Spectrum-X-Gamma (Westergaard et al. 1990) and as shown in Fig. 4 (right). The focal length of the telescope is 2 meters, constrained by the available space in the launch vehicle flaring. Each mirror is made of aluminum (thickness ~0.2 mm) with a replicated gold surface on the reflecting side, similar to the mirrors used in the Suzaku mission (Kunieda et al. 2001). The on-axis half-power diameter of the point spread function (PSF) in the focal plane is ~2 arcmin. X-ray reflectivity of the mirrors was measured at a few energies and the smoothness of the
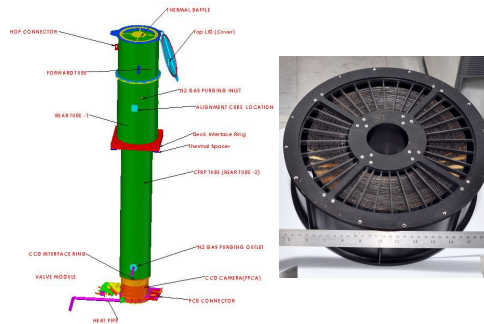
mirrors found to be in the range of 7 – 10 Å (FWHM) (Sagdeo et al. 2010). X-rays are focused on a Charge Coupled Device (CCD-22; a MOS device) housed in a Focal Plane Camera Assembly (FPCA).

The CCD-22 used in the FPCA was built by E2V Technologies Inc., UK, for the European Photon Imaging Camera (EPIC) onboard the XMM-Newton observatory. The FPCA was built in collaboration with the University of Leicester, and provides the required vacuum, low temperature and protection from the optical light and energetic protons. The optical blocking is similar to the XMM-Newton thin filter. A proton shield surrounds the CCD inside the FPCA. The CCD is cooled to 193 K (-80° C) by a thermoelectric cooler (TEC) and a radiator plate assembly. Five individual Fe^{55} radioactive calibration sources are provided in the camera, with four of these illuminating the four corners (outside the field of view) of the CCD to provide in-flight calibration at two principal line energies of ~5.9 & 6.5 keV energies. The fifth source is under the door that seals the FPCA with vacuum inside, and thus will be ineffective once the FPCA door is opened in orbit in one time operation. The on-axis (and at a few off-axis angles) effective area of the telescope, including CCD Quantum Efficiency (for isolated and bi-pixel events 1–4) and including absorption by the optical blocking filter, is shown as a function of energy in Fig. 5.

Table 1. Performance parameters of ASTROSAT

Parameter	UVIT	SXT	LAXPC	CZTI	SSM
Detector	Intensified CMOS, used in photon counting mode or integration mode	X-ray (MOS) CCD at the focal plane. (XMM & Swift heritage)	Proportional counter	CdZnTe detector array	Position-sensitive proportional counter
Imaging / non-imaging	Imaging	Imaging	Non-imaging	Imaging	Imaging
Optics	Twin Ritchey-Chretian 2 mirror system.	Conical foils (~Wolter-I) mirrors. 2-m focal length	Collimator	2-D coded mask	1-D coded mask
Bandwidth	1300-5500 Å	0.3 - 8 keV	3 - 80 keV	10-100 keV	2.5 - 10 keV
Geometric Area (cm^2)	~1100	~250	10800	1024	~180
Effective Area (cm^2)	8 - 50 (depends on filter)	~128@1.5 keV ~22@6 keV	8000@5-20 keV	1000 (E>10 keV)	~11@2 keV ~53@5 keV
Field of View (FWHM)	28' dia	~ 40' dia	1°x 1°	6°x 6°	10°x 90°
Energy Resolution	<1000 A (depends on filter)	~5-6%@1.5 keV ~2.5%@6keV	12%@22 keV	5%@100 keV	25%@6 keV
Angular Resolution	1.8 arcsec (FUV,NUV) 2.2 arcsec (Vis)	~2 arcmin (HPD)	~(1-5) arcmin (in scan mode only)	8 arcmin	~12 arcmin
Time resolution	1.7 ms	2.4 s, 278 ms	10 μs	1 ms	1 ms
Typical observation time per target	30 min	0.5 - 1 day	1 - 2 days	2 days	10 min
Sensitivity (Obs. Time)	Mag. 20 (5σ) 200 s (130-180 nm)	~ 10^{-13} erg/cm^2/s (5 σ) (20000 s)	0.1 milliCrab (3σ) (1000 s)	0.5 milliCrab (3σ) (1000s)	~28milliCrab (3σ) (600s)

5.2. Ultra-Violet Imaging Telescope (UVIT)

The UVIT will image the sky simultaneously in three broad wavelengths: FUV (130-180 nm), NUV (200-300 nm), and VIS (320-550 nm), in a circular field of ~ 28 arcmin diameter. The spatial resolution (FWHM) is < 1.8 arcsec for the FUV and NUV channels,
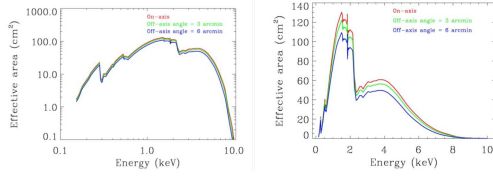
Fig. 5. Effective Area of the SXT (Left: Log scale; Right: Linear scale).

Fig. 6. Left: Schematic of the two UVIT telescopes with all major parts integrated. Right: The back-ends of the two UVIT telescopes with the detectors mounted during laboratory tests.

and ∼ 2.2 arcsec for the VIS channel. Sets of filters are mounted in filter-wheels in front of detectors for selecting narrower wavelength bands. In the two main ultraviolet channels, gratings are also provided for low-resolution (∼100) slit-less spectroscopy. The focusing optics is configured as twin Ritchey-Chretian (R-C 2) telescopes, each with a hyperbolic primary (f/4.5) mirror with effective diameter of ∼ 375 mm and overall focal length of 4750 mm. A schematic of the overall structure is shown in Fig. 6 (left). A cylindrical baffle extends over each of the telescopes for attenuating the radiation from off-axis sources. With these baffles the light reaching the detector from sources at 45° from the axis will be attenuated by a factor 10^9; for example, the light reaching the detector from full Moon at 45° from the axis will be less than the average sky background. In addition to these baffles, the doors will act as sun shades as long as the Sun is at > 45° from the axis and the plane containing the optical axis and normal to the doors. In order to avoid contamination of the optics due to ultraviolet assisted reactions, bright-earth will be kept away from the axis by >12° , and the sun behind the sun-shield at all times even if UVIT is not observing.

The three detectors in the focal plane of the UVIT are intensified CMOS type with an aperture of ∼40 mm diameter (see Fig. 6 (right) and Postma et al. 2011). A set of two micro-channels plates (MCPs) are used for multiplication of the photoelectrons. The intensified CMOS detectors can either be used in a high gain photon counting mode, or in a low gain integration mode with the multiplication kept at a low value where the raw frame of CMOS is transmitted. Typically the UV detectors are used in photon counting mode and the visible
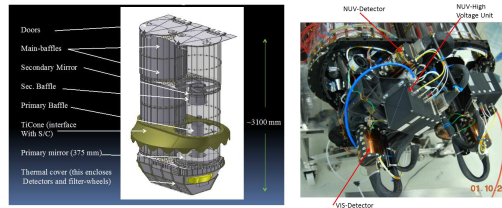
detector in integration mode. Either the entire array of 512 x 512 pixels can be read (max. rate of ∼29 frames/s), to capture the full field, or a part of the field can be read in "window" mode at rates up to ∼600 frames/s, depending on the area of the window. The effective areas as a function of the wavelengths have been estimated for all the filters and telescopes and are shown in Fig. 7.
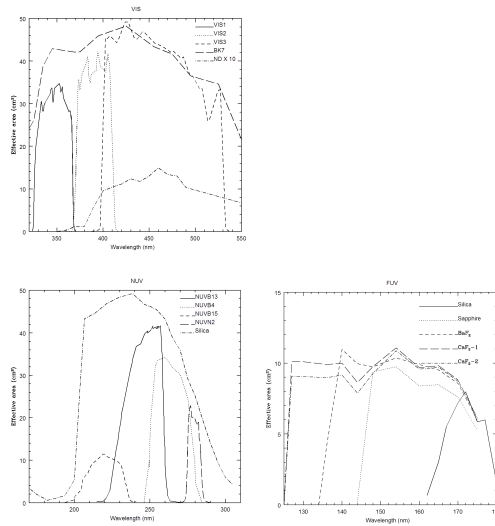

Fig. 7. Effective areas of UVIT channels with various filters. Top: Visible channel; Bottom left: NUV channel; Bottom right: FUV channel.
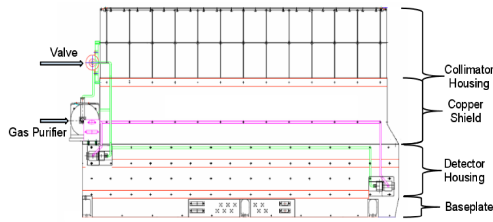
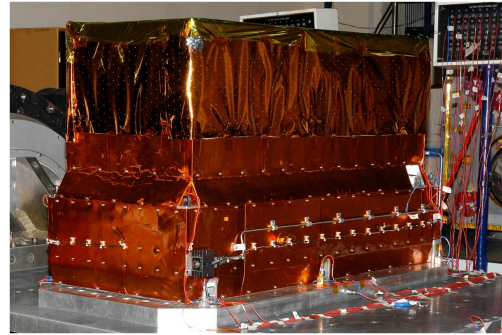**Fig. 8.** Schematic drawing of a LAXPC showing its various parts.

Fig. 9. One fully assembled and tested LAXPC unit on a vibration table.

5.3. Large Area Xenon Proportional Counter (LAXPC)

LAXPC consists of 3 identical proportional counters (PCs). Each PC has its own independent front-end electronics, HV supply, and signal processing electronics. Each PC (Figs. 8 and 9) consists of 60 anode cells arranged in 5 layers providing a 15 cm deep X-ray detection volume. Each anode layer has 12 anodes. A veto layer made up of 46 anode cells surrounds the main X-ray detection volume on 3 sides to reject events due to charged particles and interaction of high energy photons in the detector. An aluminized Mylar film of 50 microns thickness serves as the gas barrier as well as the X-ray entrance window for the detector. The detector is filled with a mixture of 90% Xenon + 10 % Methane. A gas purifier system recycles the gas in the LAXPC. The window is supported against the gas pressure by a honeycomb shaped collimator. The field of view (FOV) of the LAXPC is 1° x 1° defined by a multilayer collimator of tin, copper and aluminum placed in a collimator housing. A 1 mm thick tin sheet coated with copper surrounds each LAXPC unit and serves as the shield for X-rays entering the detector from the sidewalls.

The low energy threshold (LLD) of LAXPC has been set as 3 keV and the upper threshold (ULD) will be ~80 keV. In normal operation of LAXPC there will be two modes running simultaneously: (a) Broad Band Counting (BBC) that records the event rates in various energy bands in a selectable time bin (8 msec to 1024 msec; default value 64 msec), (b) Event Mode Data that records
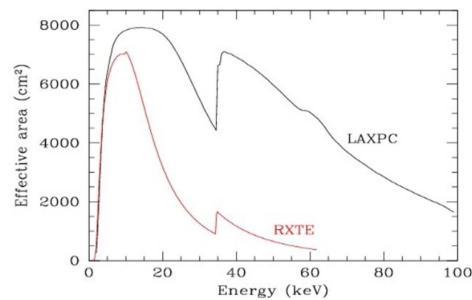

Fig. 10. Effective Area of all the 3 LAXPC units combined. Effective area of RXTE is shown (in red) for comparison.

the arrival time of each event with an accuracy of 10 msec. In addition, there is a fast counter mode in which the event rate is measured only from the top layer of each LAXPC detector in 4 energy channels covering 3-20 keV band with a fixed time bin of 160 microsecond. This mode has a dead time of ~10 msec and will be used for studying rapid variability during the short duration flares or outbursts of sources. The effective area of LAXPC as a function of photon energy is shown in Fig. 10.

5.4. Cadmium-Zinc-Telluride Imager (CZTI)

The characteristics of the CZT-Imager are given in Table 1. It has total detection area of 976 cm^2 provided by 64 CZT modules of
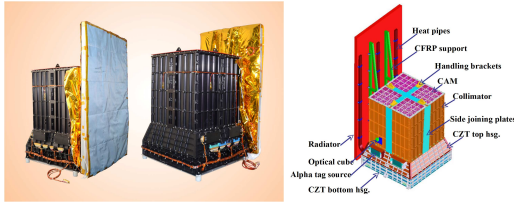
Fig. 11. Left: Two views of the fully assembled CZTI with its radiator plate. Right: Schematic showing parts of CZTI.

Fig. 12. Top Left: Schematic showing the three SSMs and their relative orientations. Top right: One fully assembled unit of SSM. Bottom: The coded mask used in an SSM.

area 15.25 cm^2 each. These 64 modules are arranged in four identical and independent quadrants. The assembled unit of CZTI, along with its schematic drawing, is shown in Fig. 11. A passive collimator (FOV of 4.6° x4.6° FWHM for photon energies < 100 keV) helps in allowing nearly parallel X-rays to enter the detector. A Coded Aperture Mask (CAM) is positioned above the collimator. The patterns are based on 255-element pseudo-noise Hadamard Set Uniformly Redundant Arrays. At energies > 100 keV the collimator slats and the coded mask become progressively transparent. For Gamma Ray Bursts, the instrument behaves like an all-sky open detector.

The CZT detectors are connected to a radiator plate that helps to maintain an operating temperature of ~0° C by passive cooling. A Cesium Iodide (Tl) based scintillator located just under the CZT detector modules and viewed by a photomultiplier tube is used for Veto measurements. A radioactive (Am^{241}) calibration source module is mounted in a gap of about 8 cm between the base of the collimator slats and the detector plane in each quadrant. This source shines alpha-tagged 60 keV photons on the CZT detector in order to calibrate the energy response.The X-ray detector has a detection efficiency of 95% within 10 – 120keV and good energy resolution (~ 8 % at 100 keV).

5.5. Scanning Sky Monitor (SSM)

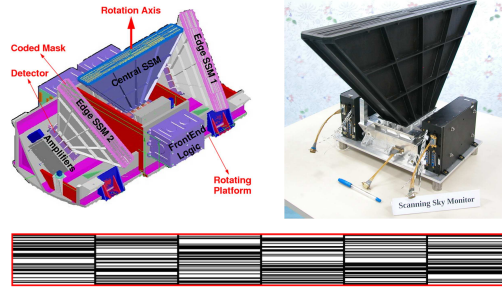SSM consists of three almost identical units of position sensitive gas-filled proportional counters with a coded-mask and associated electronics mounted on a rotating platform to scan the sky. Each unit will scan the sky in one dimension over a FOV of ~22° × 100°. Fig. 12 (left) shows a schematic of the three units of the SSM mounted on a single platform. A picture of a single unit with its electronics is also shown in Fig. 12 (right). The effective area of SSM at 5 keV is 53 cm^2(11 cm^2 at 2.5keV). Six different coded mask patterns (see Fig. 12) provide position resolution ~12 arcmin on the sky in the coding direction and 2.5° in a direction perpendicular to this. Energy resolution is 25% at 6 keV while the SSM sensitivity is ~28mCrab for a 10 min integration.

6. ASTROSAT's scientific objectives

ASTROSAT be able to carry out (a) correlated variability in soft and hard X-rays using time tagged photons data from SXT and LAXPC, (b) correlated variability in X-ray and UV bands using time tagged data from X-ray instruments and fastest possible photometric data from UVIT, (c) study simultaneous broadband X-ray spectrum from 0.3-100 keV, and perform simultaneous spectral fits, (d) search for Cyclotron absorption features (usually in ~ 10 - 60 keV energy band) in neutron star binary systems with LAXPC and CZT instruments, and (e) construct multi-frequency spectra (Spectral Energy Distributions) of variety of active galactic nuclei (AGN), stellar black hole binaries, neutron star binaries, Cataclysmic Variables (CVs), supernova remnants (SNRs)
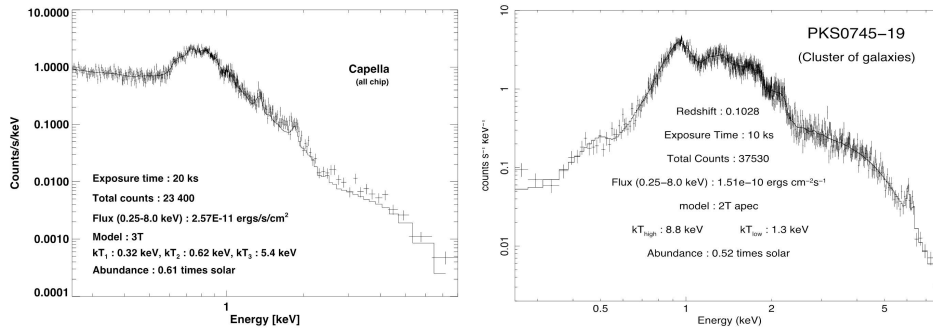
Fig. 13. Spectral simulations with SXT of a late type star: Capella (left) based on XMM-Newton archival data, and a cluster of galaxies: PKS 0745-19 based on Hicks et al. (2002) (right).

etc. The capabilities of the individual instruments towards specific astrophysical investigations are given below.

6.1. SXT

SXT will be able to: (a) resolve the K line emission from Si, S, Ar, Ca and Fe in hot thermal coronal plasmas, as well as fluorescent line emission from these elements in the medium photo-ionized by strong X-ray continuum in accretion powered X-ray sources (neutron stars, stellar mass black-holes, supermassive black-holes etc.), (b) carry out spectroscopy of hot thin plasmas in galaxies, clusters of galaxies, nuclei of active galaxies, quasars, supernova remnants and stellar coronae, (c) study the physics of shocks and accretion disks, coronae, photo-ionized regions and their density, temperature, ionization degree, and elemental abundance, (d) study low energy absorption and the nature of absorbers, for example, whether these are cold (neutral) or warm (ionized), (e) study soft X-ray excesses due to a blackbody emission in AGNs, and in binary X-ray pulsars in conjunction with other higher energy X-ray instruments, (f) carry out spatially resolved spectroscopy of Supernova Remnants and Clusters of galaxies, etc. Simulations of spectra from two types of objects – coronal emission from an active late type star and hot intra cluster gas in a cluster

of galaxies are shown in Fig. 13. Line emission components from highly ionized coronal gas can be seen clearly in these objects.

6.2. UVIT

UVIT provides many opportunities for Galactic and extra-galactic studies. The scientific aims with the UVIT are: (a) Star formation in nearby galaxies, (b) Star formation in interacting galaxies, (c) Star formation history of universe, (d) Hot stars in Globular clusters, (e) Planetary nebulae, (f) Observations of AGN simultaneous with the X-ray instruments for studies of spectral energy distributions and their temporal evolution, etc. Considering the satellite drift rate, images with UVIT will be obtained by stacking a series of sharp images obtained through short exposures and after correcting them for drift. Numerical simulations (Srivastava et al. 2009) have been carried out on images from GALEX archives to explore the effects of various observational parameters and using different centroid algorithms. An example is shown in Fig. 14.

6.3. LAXPC

High time resolution capability combined with large area and broad energy band of the LAXPC is particularly suited for the variability studies of X-ray Binaries and other cosmic
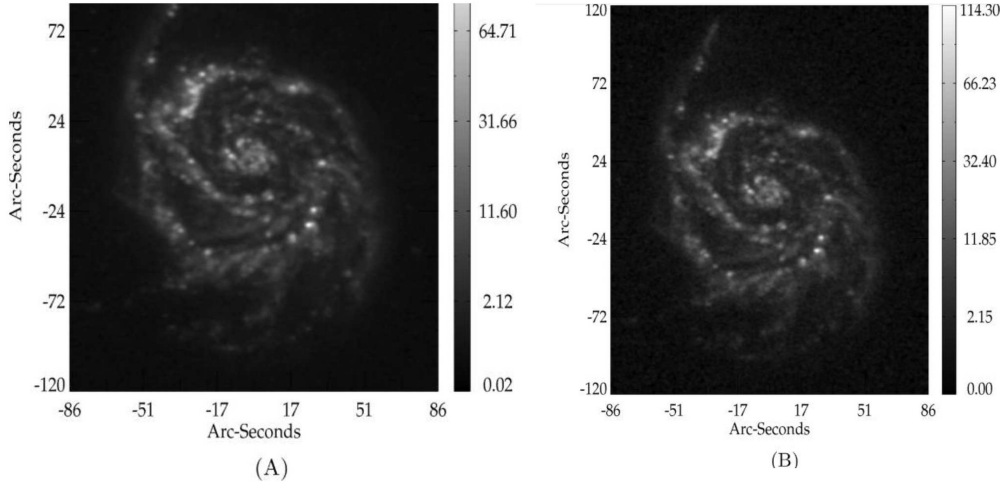
Fig. 14. Left: FUV image of M51 galaxy from GALEX after reducing the spatial scale by a factor 3 thus in effect placing the galaxy at 3 times its distance. Right: Simulated UVIT image of M51 (Srivastava et al. 2009).

sources, and measurements of spectral continuum characteristics of different classes of X-ray sources over a wide spectral band of 3-80 keV. It will be able to measure the spectral curvature and reflection components in the spectra of AGN and X-ray binary systems, Quasi-Periodic Oscillations (QPOs) at hard X-ray bands in accreting neutron star and black hole systems, cyclotron line spectroscopy of high mass X-ray binaries, and characterization of hard X-ray spectra of magnetars. Examples of spectral simulations of two blazars and two X-ray binaries are shown in Fig. 15.

6.4. CZTI

CZTI extends the high energy limit (bandwidth: 10 – 100 keV) and thus apart from the spectral studies afforded by the LAXPC it will also be able to detect gamma ray bursts and study their early light curves. See also examples in Fig. 15.

6.5. SSM

Long term X-ray behavior of transient X-ray sources like binary systems, and other very bright sources like AGN will be the focus of the SSM, apart from the discovery of the transient sources towards which the entire ASTROSAT can be pointed.

6.6. Broad-band simulations of spectra

Data from simultaneously observed sources will be amenable to joint spectral analysis. Simultaneous observations in all the four instruments will provide the spectral energy densities (SEDs) that are particularly important for AGN. Examples of SED in X-rays with three instruments for a blazar: 3C454.3, an enigmatic object that has the characteristics of both a narrow-line Seyfert galaxy and a blazar, and 1H0323+342, are shown in Fig. 15. The simulation of 3C454.3 is based on observations reported by Wehrle et al. (2012), whereas the simulation of 1H0323+342 is based on our analysis of the Suzaku archival data. Multiple components of continuum in X-ray binaries will be easy to resolve with simultaneous broadband observations as shown in Fig. 15 for 4U 1636-536, and for cyclotron line feature from high magnetic field neutron star in X-ray binary, e.g. Her X-1.
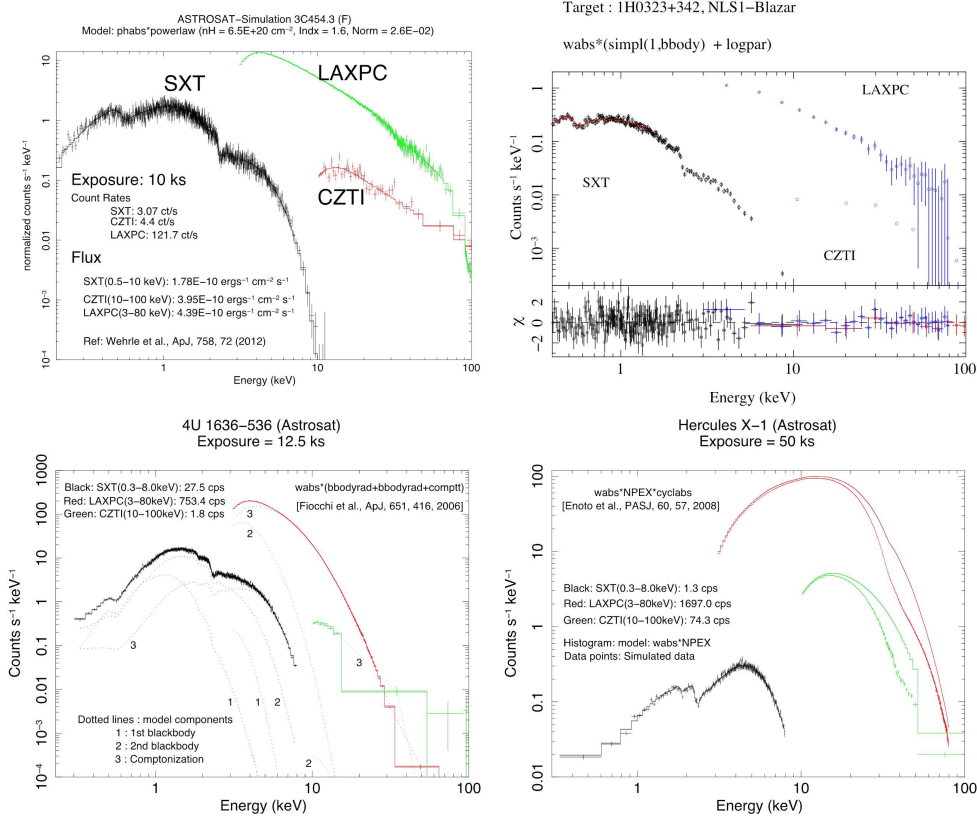
Fig. 15. Wide-band X-ray spectral simulations. Top left: Blazar 3C454.3 based on Wehrle et al. (2012). Top right: a gamma-ray bright narrow-line Seyfert 1 galaxy (1H0323+342) with an exposure time of 50 ksec. Bottom left: LMXB 1636-536 with the spectral parameter values are taken from Fiocchi et al. (2006) but with the normalization reduced by factor of 2.5 to account for reduced intensity since then. Bottom right: Her X-1 showing the cyclotron absorption line feature (Enoto et al. 2008).

7. Summary

We have discussed the capabilities of instrumentation on both SALT and ASTROSAT in the context of multi-wavelength and time variability studies of accretion driven sources across many object classes, from stellar systems to AGN. This provides some background and rationale to the planned coordinated SALT-ASTROSAT program of contemporaneous observations of such objects following ASTROSAT's launch in 2015. This project involves a number of astronomers in both South Africa and India and is supported by a recently approved India-South Africa bilateral science program.

References

Bramall, D. G., et al. 2010, Proc. SPIE, 7735, 77354F

Barnes, S. I., et al. 2008, Proc. SPIE, 7014, 70140K

Buckley, D.A.H., Swart, G. P., and Meiring, J.G. 2006a, Proc. SPIE, 6267, 32

Buckley, D.A.H., et al. 2006b, Proc. SPIE, 6269, 62690A

Burgh, E., et al. 2003, Proc. SPIE, 4841, 1463

Enoto, T., et al. 2008, PASJ, 60, 57

Fiocchi, M., et al. 2006, ApJ, 651, 416

Hicks, A.M., et al. 2002, ApJ, 580, 763

Kunieda, H., et al. 2001, Appl. Opt., 40, 553

Postma, J., Hutchings, J.B., and Leahy, D. 2011, PASP, 123, 833

Sagdeo, A., et al. 2010, Exp. Astron., 28, 11

Srivastava, M. K., Prabhudesai, S. M., Tandon, S. N. 2009, PASP, 121, 621

Wehrle, A. E., et al. 2012, ApJ, 758, 72

Westergaard, N. J., et al. 1990, Optical Engineering, 29, 658